ELSEVIER

Contents lists available at ScienceDirect

# Geoenergy Science and Engineering

journal homepage: www.sciencedirect.com/journal/geoenergy-science-and-engineering





# Transport of Ba, Sr, Cd, Pb, and As in dolomite saline aquifers injected with petroleum produced water

Khalid Omar, Javier Vilcáez

Boone Pickens School of Geology, Oklahoma State University, Stillwater, OK, 74078, USA

#### ARTICLE INFO

Keywords:
Produced water
Dolomite
Toxic metals
Sorption reactions
Precipitation reactions

#### ABSTRACT

Predicting the transport of toxic metals in dolomite saline aquifers where petroleum produced water (PW) is commonly injected is important to prevent underground sources of drinking water contamination. This study presents new experimental results on the degree and impact of precipitation and sorption reactions on the transport of high concentrations of toxic metals (80-100 mg-Ba/L, 80-100 mg-Sr/L, 70-100 mg-Cd/L, 2-100 mg-Pb/L, and 80-100 mg-As/L) in dolomite injected with PW of variable alkalinity (0-200 mg/L), total dissolved solids (1700-77,000 mg/L), and pH (2-7). Changes in the elemental and mineral composition of dolomite surface were measured by BSEs SEM, SEM-EDS, and high-resolution XRD analyses. The results reveal a key role of alkalinity generated from the dissolution of dolomite. We show that a short initial stage where the removal of toxic metals is driven by the initial pH and alkalinity of PW is followed by a prolonged stage where the removal of toxic metals by sorption and precipitation reactions is driven by the alkalinity and pH that results from the kinetic dissolution of dolomite. Precipitated/coprecipitated metals were carbonate minerals reflecting the metal composition of PW. Attained removal levels of tested toxic metals from 1 L of PW using a dolomite core made of 200~g were >90% for Pb, >50% for As, >30% for Cd, and >5% for Ba and Sr. Apparently, the in-situ generation of alkalinity (carbonate ions) and sorption reactions of metals on dolomite catalyzes the precipitation of toxic metals as carbonate minerals. This catalytic effect of dolomite is different with PW and fresh water (FW) of low salinity (NaCl). Precipitation reactions are more prominent with FW than with PW, whereas sorption reactions are more prominent with PW than with FW.

#### 1. Introduction

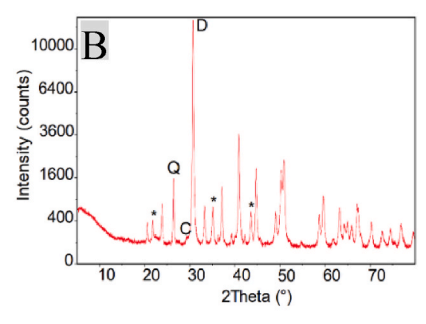
Wastewater from conventional and unconventional oil and gas industries commonly called produced water (PW) is characterized by high concentrations of total dissolved solids (TDS), dissolved organics, and dissolved gases. TDS mainly consists of chloride, carbonate, and sulfate salts of heavy metals, metalloids, and alkaline earth metals, as well as naturally occurring radioactive materials (NORM). Dissolved organics is mainly dissolved hydrocarbons and dissolved gases are mostly CO<sub>2</sub>, CH<sub>4</sub>, and H<sub>2</sub>S. Opposite to dissolved organics, heavy metals, metalloids, and alkaline earth metals are not biodegradable, and they tend to accumulate in living tissue causing serious health problems in both animals and humans (Tabatabaeefar et al., 2020). Among all metals and metalloids in PW, Pb, Cd, As, Ba, and Sr are of special concern due to their severe toxicity (Kharaka et al., 2007; Yin et al., 2019). The maximum contaminant levels (MCLs) for Pb, Cd, As, Ba, and Sr in drinking water, according to the U.S. Environmental Protection Agency

(USEPA) are 15  $\mu$ g/L, 5  $\mu$ g/L, 10  $\mu$ g/L, 2000  $\mu$ g/L, and 0.1 pCi/L, respectively (Guerra et al., 2011).

Considering that the global volume of offshore PW in the world has been reported to be 39.5 Mm<sup>3</sup>/day (Jiménez et al., 2018) and that concentrations of toxic metals and metalloids in PW in the orders of mg/L (Alomar et al., 2022), the spill of small amounts of PW can lead to the contamination of huge volumes drinking groundwater. Therefore, for safety and economic motives, PW is sometimes injected into deep dolomite saline aquifers (Walsh and Zoback, 2015). However, the injection of huge volumes of PW into geologic units still raises the prospect of underground sources of drinking water (USDW) contamination due to the possible upward migration of PW through induced or naturally occurring faults, fractures, and abandoned wells. This prospect along with limited information on the transport of concentrations of toxic metals and metalloids in the order of mg/L at salinity levels of PW in dolomite aquifers motivated the overall objective of this study, which is to develop an understanding of the transport of toxic metals and

E-mail address: vilcaez@okstate.edu (J. Vilcáez).

<sup>\*</sup> Corresponding author.



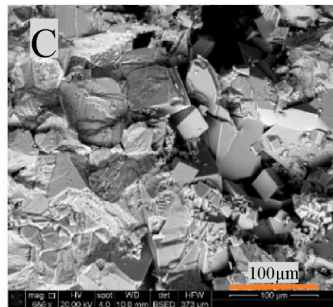


Fig. 1. A) Thin section (scale bare  $=200~\mu m$ ) showing shape and size of dolomite crystals, B) XRD analysis showing that the employed dolomite rocks are mainly composed of dolomite (represented by D only on the 104-dolomite peak) with minor quantities of quartz and calcite cement (represented by Q only on the 101-quartz peak, and C only on the 104-calcite peak which is very weak). Dolomite cations (e.g., Mg & Ca) ordering reflections are indicated by asterisks on 101, 015 and 021 dolomite peaks. C) SEM image showing the shape and size of dolomite crystals as well as porosity.

 Table 1

 Initial composition of the synthetic produced waters (PW).

	Type of produced waters (PW)					
(mg/L)	I	II	III	IV		
Na	15943.5	16957.8	17,273.40	17935.3		
Cl	31310.5	31353.5	41,965.50	43536		
Ca	4014.7	4191.6	7175.5	7484.3		
Mg	940.2	974.3	1011.9	815.6		
Ba	90.3	87	97.7	79.9		
Sr	91.3	88.3	102.1	81.9		
Cd	71.3	61.1	97.6	72.8		
Pb	3.8	3.9	67.3	81.1		
As	93.3	83.8	93.6	84.4		
Alkalinity	101.7	79.6	O <sup>a</sup>	0 <sup>a</sup>		
pН	6.9	6.9	2.61	2.1		

<sup>&</sup>lt;sup>a</sup> Below detection limit.

**Table 2** Initial composition of synthetic freshwaters (FW).

	Type of freshwater (FW)		
(mg/L)	I	II	
Na	31.2	38.3	
Cl	436.6	607.1	
Ca	100.4	45.6	
Mg	11.2	21.9	
Ba	97	98.2	
Sr	101	99.1	
Cd	95.8	99.4	
Pb	33.7	99	
As	95.8	106.8	
Alkalinity	2.8	O <sup>a</sup>	
pН	6	2.7	

<sup>&</sup>lt;sup>a</sup> Below detection limit.

metalloids in dolomite at salinity levels of PW. Several studies have already been conducted to analyze the reactivity of trace ( $\mu g/L$ ) concentrations of toxic metals and metalloids in shallow groundwater. This study deals with high (mg/L) concentrations of toxic metals and metalloids in dolomite saline aquifers.

In a previous study we conducted batch reaction experiments to elucidate the role of alkalinity on the removal of Ba, Sr, Cd, Pb, and As from PW by sorption and precipitation reactions on dolomite grains. The results indicated that under high alkalinity conditions and salinity levels of PW, Ba, Sr, Cd, Pb, and As undergo both sorption and precipitation reactions, with Ba, Sr, and Cd undergoing mostly sorption reactions and Pb and As undergoing mostly precipitation reactions (Omar and Vilcáez, 2023). Moreover, we found that the rate of toxic metals removal by mineral precipitation reactions is proportional to the dissolution rate of dolomite which provides carbonate and bicarbonate ( $CO_3^2$  and  $HCO_3$ )

ions and cations (Ca and Mg) that compete for the sorption sites of dolomite (Ebrahimi and Vilcáez, 2018a, 2018b, 2019). Building on this knowledge, this study aims to elucidate the effect of both sorption and precipitation reactions on the transport of high concentrations of Ba, Sr, Cd, Pb, and As in dolomite, at variable alkalinity conditions and salinity levels of PW.

Sorption reactions of cations on minerals like dolomite can be due to physical, electrostatic, and chemical interactions (Drever, 1997), Physical interactions are the attraction between ions and mineral surfaces due to Van Der Waals forces. Whereas electrostatic interactions are the attraction of cations and negatively charged sites on mineral surfaces. Chemical interactions are chemical bonds between ion molecules and one or more atoms on mineral surfaces. Generally, sorption reactions are the most important interactions affecting the transport of contaminants in groundwater. Therefore, understanding these interactions (physical, electrostatic, and chemical) is important to predict the transport of toxic metals and metalloids in dolomite saline aquifers where PW is commonly disposed. However, precipitation reactions of carbonate, silicate, and sulfate minerals can also affect the transport of toxic metals in dolomite if the solubility product of the mineral is exceeded and the kinetics of the reaction is favorable. Numerous previous studies have been conducted to understand the transport of toxic metals and metalloids in reactive porous media (e.g., graphite oxides, quartz sand, iron oxide sediments) (Jensen, 2020; Saha et al., 2020; Yin et al., 2019). However, a study to understand the effect of sorption and precipitation reactions on the transport of Ba, Sr, Cd, Pb, and As concentrations in the order of mg/L in dolomite, at variable alkalinity and salinity levels of PW has not been done before. Our approach to bridge this knowledge gap consisted of core-flooding experiments using synthetic dolomite cores made of compressed dolomite grains of the same size and synthetic PW composed of the same elements. The use of synthetic dolomite cores of the same surface area and flow and transport properties (e.g., permeability, dispersivity, and tortuosity), and PW of the same elements is to be able to conduct reproducible experiments and to be able to focus on the transport process of the selected toxic metals and metalloids. For the sake of comparisons and to assess the effect of salinity and pH, synthetic freshwater (low salinity water), and acidic PW are included in the experiments.

The results of this study are presented in terms of the removal profiles of toxic metals under different alkalinity and salinity levels, as well as in terms of the changes in the elemental and mineral composition of dolomite surface due to precipitation and sorption reactions. For the sake of readability, in this work, Ba, Sr, Cd, Pb, and As are called toxic metals, and alkalinity refers to the concentration of carbonate and bicarbonate ions.

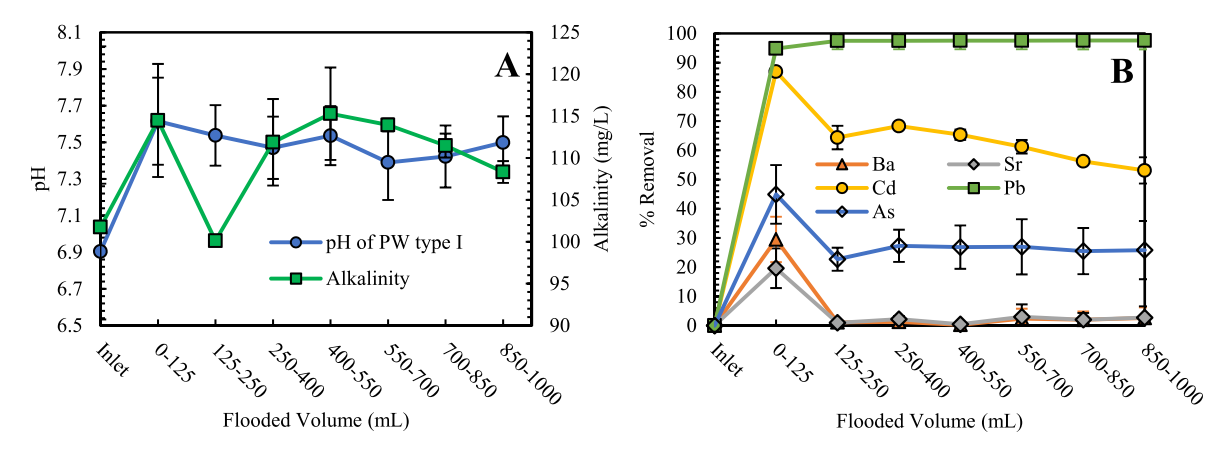


Fig. 2. Toxic metals removal from PW type I (added with CaCO<sub>3</sub>) using a 16.9 cm dolomite core: A) pH and alkalinity profiles at the outlet of the dolomite core, and B) Toxic metals removal profiles at the outlet of the dolomite core.

Table 3
Toxic metals removal from PW.

	Type of produced water (PW)			
	I	II	III	IV
Final pH	7.57	7.51	7.2	7.37
Alkalinity increment (mg/L)	6.59	-8	$0^a$	$0^a$
Ba removal (%)	3.45	2.86	4.43	1.34
Sr removal (%)	2.8	0.36	2.59	1.06
Cd removal (%)	64.77	44.86	44.81	11.89
Pb removal (%)	96.42	94.89	97.57	95.89
As removal (%)	28.26	17.17	29.19	25.42

I and III: Used with 8.1 cm dolomite core length..

II and IV: Used with 16.2 cm dolomite core length..

#### 2. Materials

#### 2.1. Dolomite

Arbuckle Group dolomite was collected from the outcrop in southwest Missouri. To confirm the purity of dolomite, samples were analyzed via Powder X-ray Diffraction (Bruker XRD D8 ADVANCE Plus) analysis. The analysis confirmed that samples were composed of 98% dolomite and 2% of both blocky calcite and silica cement. The XRD spectrum distinguished dolomite-structure (JCPDS: 79–1342) from calcite structure (JCPDS: 86–2334) minerals by displaying the highest intensity of 104 (>2500 counts) at 31 $^{\rm o}$ 2  $\Theta$  as well as the strong dolomite cation (e.

g., Mg and Ca) ordering peaks (101, 015, and 021 at  $22^{\circ}$   $2\Theta$ ,  $35^{\circ}2\Theta$ , and  $44^{\circ}2\Theta$ , respectively). The samples are near perfect dolomite and thus have near stochiometric composition (Mg/Cã1). Our petrographic analysis demonstrated that the dolomite crystals vary between planar euhedral to subhedral, and non-planner which are in agreement with previous studies done on the Arbuckle Group dolomite in Missouri and Oklahoma (Temple et al., 2020). Our analysis also showed different crystal sizes ranging between 5  $\mu$ m and 0.6 mm (Fig. 1).

#### 2.2. Synthetic dolomite core

The collected dolomite was crushed and sieved multiple times to obtain dolomite grains of 300–600  $\mu m$  size. Prior to their utilization, dolomite grains were washed with ultrapure deionized water in an ultrasonic bath to remove dust particles. The prepared dolomite grains were used to make synthetic dolomite cores. Firstly, 200 g of dried powdered dolomite and 10 g of ultrapure deionized water was placed in the beaker then mixed very well. Secondly, the resulting aggregate was put into a stainless-steel cylindrical mold. Next, the mold was placed inside a uniaxial compaction apparatus (Carver Laboratory Presser (Model 4387)) exerting a pressure of 4320 psi for 1 h. The dimensions of the resulting synthetic dolomite core were 3.8 cm diameter and  $\sim\!\!8.1$  cm length with porosity and permeability of 15% and 1000 mD, respectively. Finally, one or two of these filters were placed into the core holder of a core-flooding system to conduct the experiments using synthetic PW or freshwater.

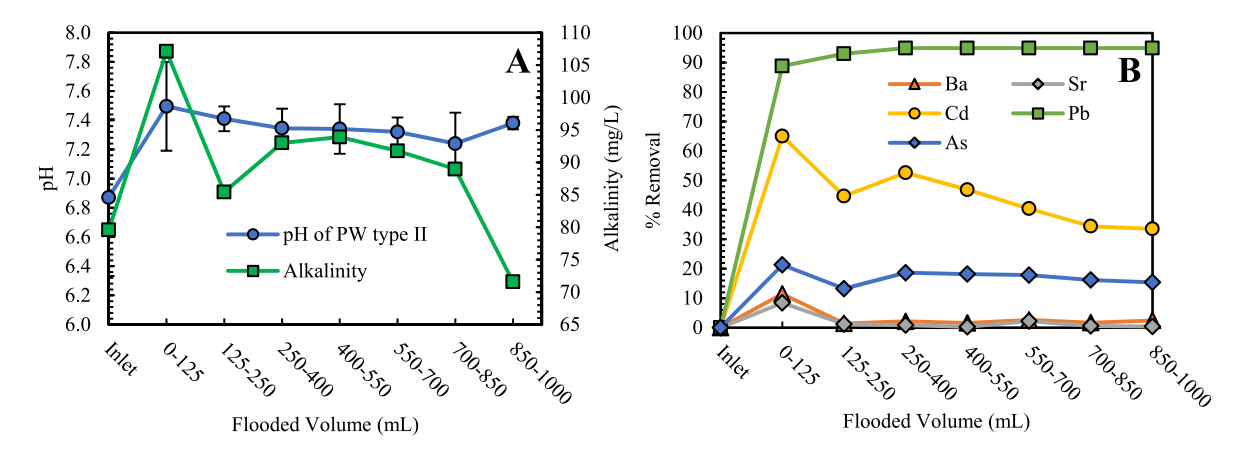


Fig. 3. Toxic metals removal from PW type II (added with CaCO<sub>3</sub>) using an 8.2 cm dolomite core: A) pH and alkalinity profiles at the outlet of the dolomite core, and B) Toxic metals removal profiles at the outlet of the dolomite core.

<sup>&</sup>lt;sup>a</sup> Below detection limits.

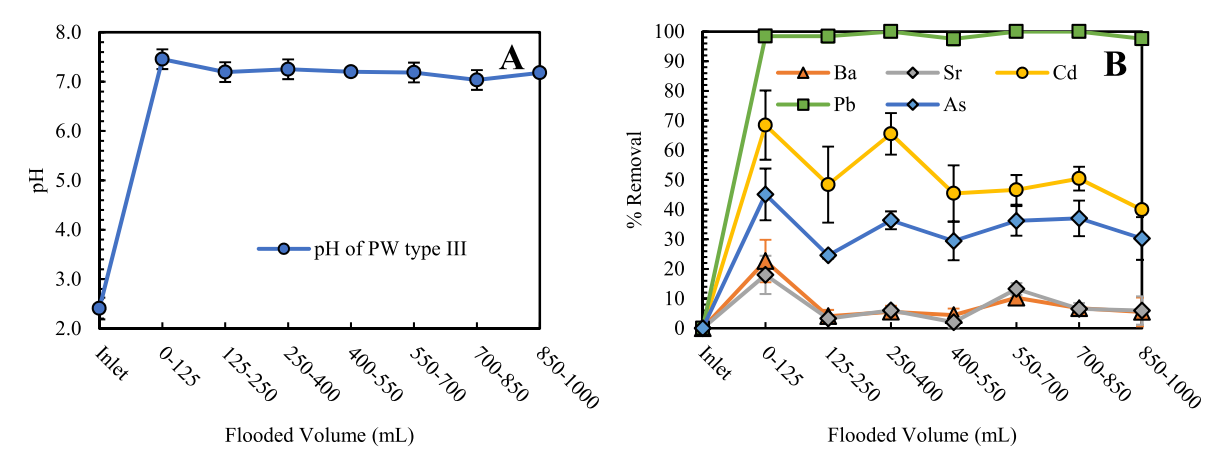


Fig. 4. Toxic metals removal from PW type III (not added with CaCO<sub>3</sub>) using a 15.8 cm dolomite core: A) pH profile at the outlet of the dolomite core, and B) Toxic metals removal profiles at the outlet of the dolomite core.

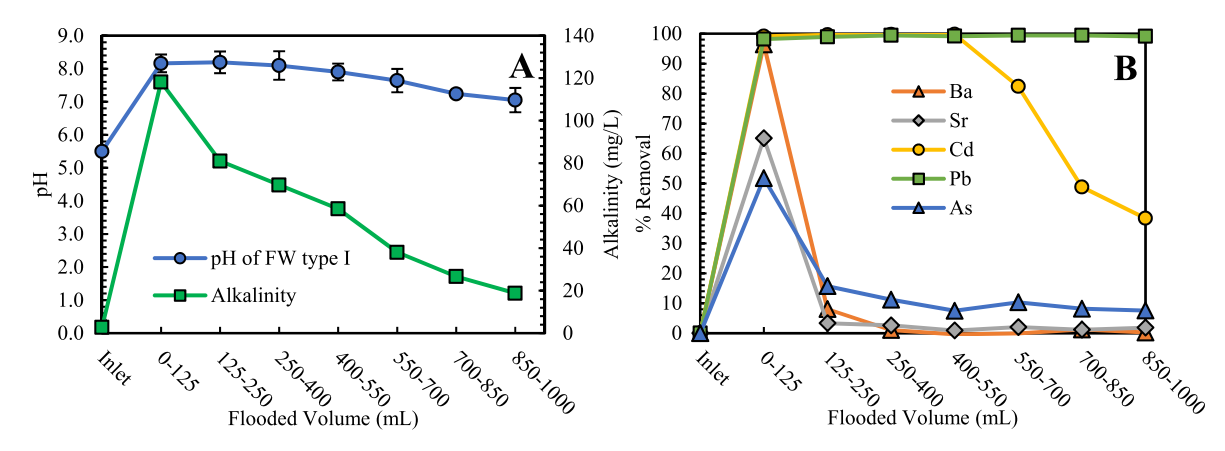


Fig. 5. Toxic metals removal from FW type I (added with CaCO<sub>3</sub>) using a 15.8 cm dolomite core: A) pH and alkalinity profiles at the outlet of the dolomite core, and B) Toxic metals removal profiles at the outlet of the dolomite core.

Table 4
Toxic metals removal from FW.

	Type of freshwater (FW)		
	I	II	
Final pH	7.59	7.85	
Alkalinity increment (mg/L)	16.04	32.84	
Ba removal (%)	11.79	16.46	
Sr removal (%)	7.59	11.13	
Cd removal (%)	85.61	94.42	
Pb removal (%)	99.41	99.98	
As removal (%)	11.79	18.51	

I and II: Used with 16.2 cm dolomite core length.

## 2.3. Synthetic produced water

Since TDS in PW is composed of chloride and carbonate salts (Guerra et al., 2011), synthetic PW was prepared by adding NaCl, CaCl<sub>2</sub>.2H<sub>2</sub>O, MgCl<sub>2</sub>.6H<sub>2</sub>O, SrCl<sub>2</sub>.6H<sub>2</sub>O, BaCl<sub>2</sub>.2H<sub>2</sub>O, Cd(CO<sub>3</sub>)<sub>2</sub>.4H<sub>2</sub>O, PbCl<sub>2</sub>, and AsCl<sub>3</sub> (Fisher Scientific Co. with the purity of >99.9%) into ultrapure deionized water (Table S1). TDS of the prepared synthetic PW was 69, 200–77,300 mg/L. To confirm the different behavior of the tested toxic metals in PW (high salinity water) and freshwater (low salinity water), synthetic freshwater (FW) was prepared and used to conduct the same experiments as with synthetic PW. TDS of the prepared synthetic FW was <1700 mg/L and contained the same salts as the synthetic PW (Table S2). The initial alkalinity of the prepared synthetic PW and FW

that resulted from the dissolution of atmospheric  $CO_2$ , was increased by adding  $CaCO_3$ . To maximize the dissolution of the added salts, the prepared synthetic PW and FW were stirred overnight. Possible undissolved particles in the prepared synthetic PW and FW were removed by filtration using a 0.4  $\mu$ m cellulose filter. Different types of synthetic PW and FW were prepared. PW types I and II were added with  $CaCO_3$  to increase alkalinity, whereas PW types III and IV were not added with  $CaCO_3$ . Likewise, FW type I was added with  $CaCO_3$  to increase alkalinity, whereas FW type II was not added with  $CaCO_3$ .

We used concentrations of Ca and Mg in the synthetic PW that correspond to PW in Oklahoma (Ribeiro et al., 2021) and U.S. Mid Continent (Guerra et al., 2011). Since concentrations of sulfate in PW are negligible in these regions, sulfate is not considered in this work. Therefore, the prepared synthetic PW and FW did not contain sulfate. By not including sulfate we also eliminated a source of uncertainty as sulfate can precipitate Ba. Arsenite (As (III)) salt (AsCl<sub>3</sub>) was used instead of arsenate (As(IV)) because PW originates under reduced conditions and the oxidation of arsenite to arsenate by dissolved oxygen is very slow (Dixit and Hering, 2003). To be able to assess the competition for hydration sites of dolomite and precipitation as carbonate minerals of Ba, Sr, Cd, Pb, and As, we added 100 mg/L (Alomar et al., 2022) of each of these toxic metals and metalloids to the prepared synthetic PW and FW (Tables S1 and S2). However, their concentrations differed depending on their solubility at tested alkalinity and pH conditions (Tables 1 and 2). We included synthetic PW of low pH ( $\sim$ 2.0) (PW types III and IV, and FW type II) to increase the rate of dolomite and thus the generation of alkalinity from the dissolution of dolomite. To obtain a low pH we used

Fig. 6. SEM images of toxic metals precipitates (bright white) on dolomite surface: A) Control sample, B) Flooded with FW type II, C) Flooded with PW type II (inlet).

As(III) dissolved in hydrochloric acid.

#### 3. Methods

The analytical methods we used to analyze the effect of precipitation and sorption reactions on the transport of Ba, Sr, Cd, Pb, and As in dolomite consisted of X-ray Powder Diffraction (XRD), Scanning Electron Microscopy-Dispersive X-ray Spectroscopy (SEM-EDS), and backscattered electrons (BSEs) SEM analyses of dolomite grains surfaces. XRD is commonly used to analyze the mineral composition of dry rock grains, including crystal and amorphous carbonate phases (Wei et al., 2003). XRD in this study is used to determine the nature and mineral composition of carbonate precipitates. BSEs-SEM and SEM-EDS are cutting-edge technologies used to show the morphology of grains/crystals at the nano-scale level. They enable the elemental classification of particles. In this study, SEM-EDS and BSEs-SEM are used to map the elemental composition and morphology of sorbed and precipitated elements on dolomite. During BSEs SEM imaging, materials are shot with high energy (eV). Elements with higher density can reflect more energy back to the detector. Thus, BSEs-SEM can differentiate rock minerals based on the density of their elements, the denser the elements in the mineral, the brighter the mineral will be displayed in the SEM image. For instance, the density of dolomite (2.87 g/cm<sup>3</sup>) is higher than calcite (2.71 g/cm<sup>3</sup>). Therefore, calcite shows higher brightness than dolomite in the BSEs SEM image due to the higher Ca content in calcite than in dolomite.

#### 3.1. Core-flooding experiments

Core-flooding experiments consisted of injecting 1 L of synthetic PW and FW into the prepared dolomite core placed in a Hassler Type coreholder (RCH-series of Core Laboratory). Confining pressure in the coreholder was 2300 psi. The injection operation was done using a floating piston accumulator connected to a 260 dual syringe pump (Teledyne ISCO). Water was injected at a constant flow rate of 0.1 mL/min through two inlet points at the bottom of the core-holder. The inlet pressure was monitored by the pressure transducer of the syringe pump. Water samples were collected at the inlet and outlet of the core holder. Their compositions were analyzed at the Soil, Water, and Forage Analytical Laboratory (SWFAL) of Oklahoma State University. The analysis included the measurement of all heavy metals, alkaline earth metals, and metalloids of interests (Na, Ca, Mg, Ba, Sr, Cd, Pb, and As), chloride (Cl<sup>-</sup>), pH, and total alkalinity (CO<sub>3</sub><sup>2-</sup> and HCO<sub>3</sub>). The concentration of Na, Ca, Mg, Ba, Sr, Cd, Pb, and As were measured by ICP-OES analysis. Alkalinity was measured by the titration method using a Hach TitraLab AT1000 Series auto-titrator with an autosampler. This method involves the titration of samples with standard 0.02N sulfuric acid (H2SO4) titrant to endpoints of pH 8.3 and 4.5. The pH endpoint of 8.3 corresponds to carbonate alkalinity, whereas the pH endpoint of 4.5 corresponds to bicarbonate alkalinity. Chloride was measured by the colorimetric method using ferricyanide in a flow-injection analyzer (Ballinger, 1979; Federation and Aph Association, 2005). At the end of the experiments, dolomite grains (~3g) were sampled from the bottom (inlet), center, and top (outlet) of the dolomite core (Fig. S1) for BSEs SEM, XRD, and SEM-EDS analyses to determine changes in the morphology as well as the elemental and mineral composition of the dolomite grains surface due to precipitation/dissolution sorption/desorption reactions. For the sake of results validation, experiments were repeated at least two times. Tables 1 and 2 show the measured alkalinity, initial pH, and composition of all synthetic PW and FW used to conduct the core-flooding experiments.

#### 3.2. XRD, BSEs SEM, and SEM-EDS analyses

To determine the effect of sorption and precipitation reactions on the transport of toxic metals in dolomite, we used BSEs SEM, SEM-EDS and XRD analyses. BSEs SEM analysis was used to identify changes in the surface morphology of the dolomite grains due to dissolution/precipitation reactions and to examine the amorphous and/or crystalline phases of precipitated metals. SEM-EDS was used to map the elemental distribution (sorption/precipitation of toxic metals) on the surface of dolomite. Dolomite samples were dried but not pulverized for BSEs SEM and SEM-EDS analyses. This analysis was performed at the OSU Microscopy Laboratory using a SEM FEI Quanta 600 field emission gun ESEM with Bruker EDS and HKL EBSD. Samples for SEM-EDS analysis were coated with carbon (graphite) to prevent artifacts and to optimize the quality of the microphotographs. To avoid missing any relevant features and enhance the generated results, SEM-EDS mapping was performed at different magnification scales (e.g., 1 mm, 100 µm, and 10  $\mu m$ ). Same samples that were used for SEM-EDS analysis were used for conducting BSEs SEM analysis. Since SEM-EDS analysis provides compositional information about the composition of crystalline and amorphous phases of precipitates, we used powder XRD to distinguish the amorphous and crystalline nature of the precipitates. XRD is commonly used for identifying mineral crystals and their polymorphs in rocks. A quantitative application of this analytical method presents several challenges and limitations. Thus, we performed a semiquantitative analysis using data obtained from high resolution XRD analysis on pulverized dolomite grains at the Microscopy Laboratory of Oklahoma State University (using Bruker D8 ADVANCE Plus XRD). The semi-quantitative analysis was achieved via DIFFRAC.EVA software using the ICDD-PDF-2-2022 and Crystallography Open Database (COD).

#### 4. Results and discussion

Core-flooding experiments were conducted to analyze the effect of precipitation and sorption reactions on the transport of Ba, Sr, Cd, Pb, and As in dolomite. To this aim we measured the removal levels of Ba, Sr, Cd, Pb, and As by the dolomite cores, and we analyzed changes in the morphology, as well as in the elemental and mineral composition of the

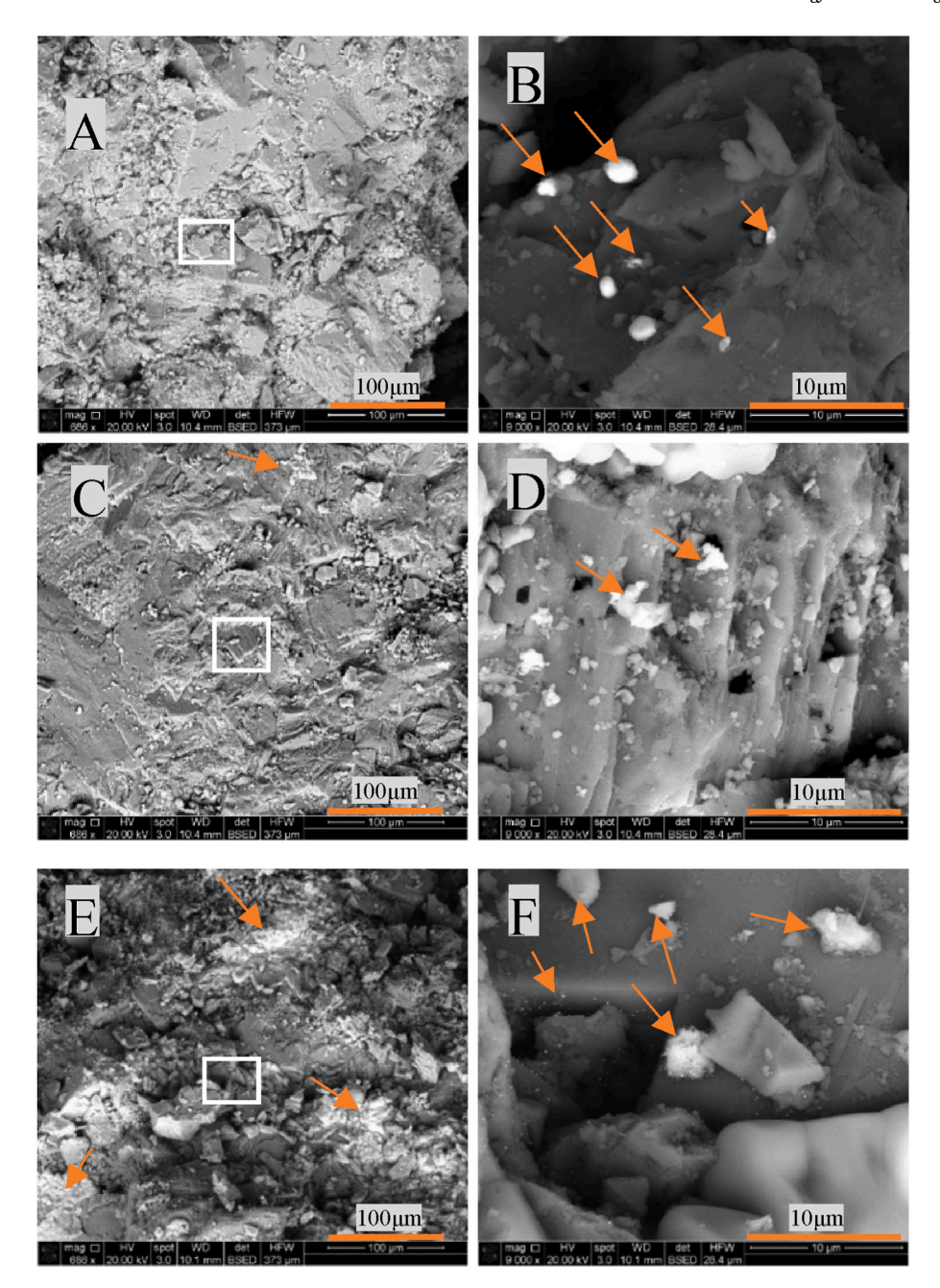


Fig. 7. SEM images of toxic metals precipitates (bright white) on dolomite surface with PW type I (added with CaCO<sub>3</sub>): A) Inlet of the dolomite core, B) Zoom-in of A, C) Center of the dolomite core, D) zoom-in of C, E) Outlet of the dolomite core showing huge bright patches of precipitates, and F) zoom-in of E showing precipitates of different size and shapes.

dolomite grains collected from different points in the dolomite core after each core-flooding experiment. The core-flooding experiments consisted of injecting 1 L of PW and FW into synthetic dolomite cores. We used two lengths of dolomite cores ( $\sim$ 8.1 and  $\sim$ 16.2 cm length).

#### 4.1. Removal of toxic metals

Fig. 2 shows Ba, Sr, Cd, Pb, and As removal profiles, as well as total alkalinity concentration and pH profiles at the outlet of the dolomite core (16.9 cm length) injected with PW type I of  $102\ mg/L$  total alkalinity (Table 1). Lower concentrations of all toxic metals at the outlet than at the inlet confirm their removal by dolomite due to precipitation and sorption reactions (see Table 3).

A higher removal level of all toxic metals at the beginning than at the subsequent stages of the flooding process is attributed to a transition

stage where sorption and precipitation reactions are controlled by the initial alkalinity and pH of PW, to a stage where sorption and precipitation reactions of toxic metals is controlled by the alkalinity and pH that results from the dissolution of dolomite according to the following reaction mechanism (Vilcáez, 2020):

Dolomite dissolution:

$$CaMgCO_3 + 2H^+ \leftrightarrow Ca^{2+} + Mg^{2+} + 2HCO_3^-$$
 (1)

$$HCO_3^- \leftrightarrow H^+ + CO_3^{2-} \tag{2}$$

Sorption reactions (Pokrovsky et al., 1999):

$$> CO_3H^{\circ} + Ms^{2+} \leftrightarrow > CO_3Ms^{+} + H^{+}$$
 (3)

$$> MeOH^{o} + H^{+} \leftrightarrow > MeOH_{2}^{+}$$
 (4)

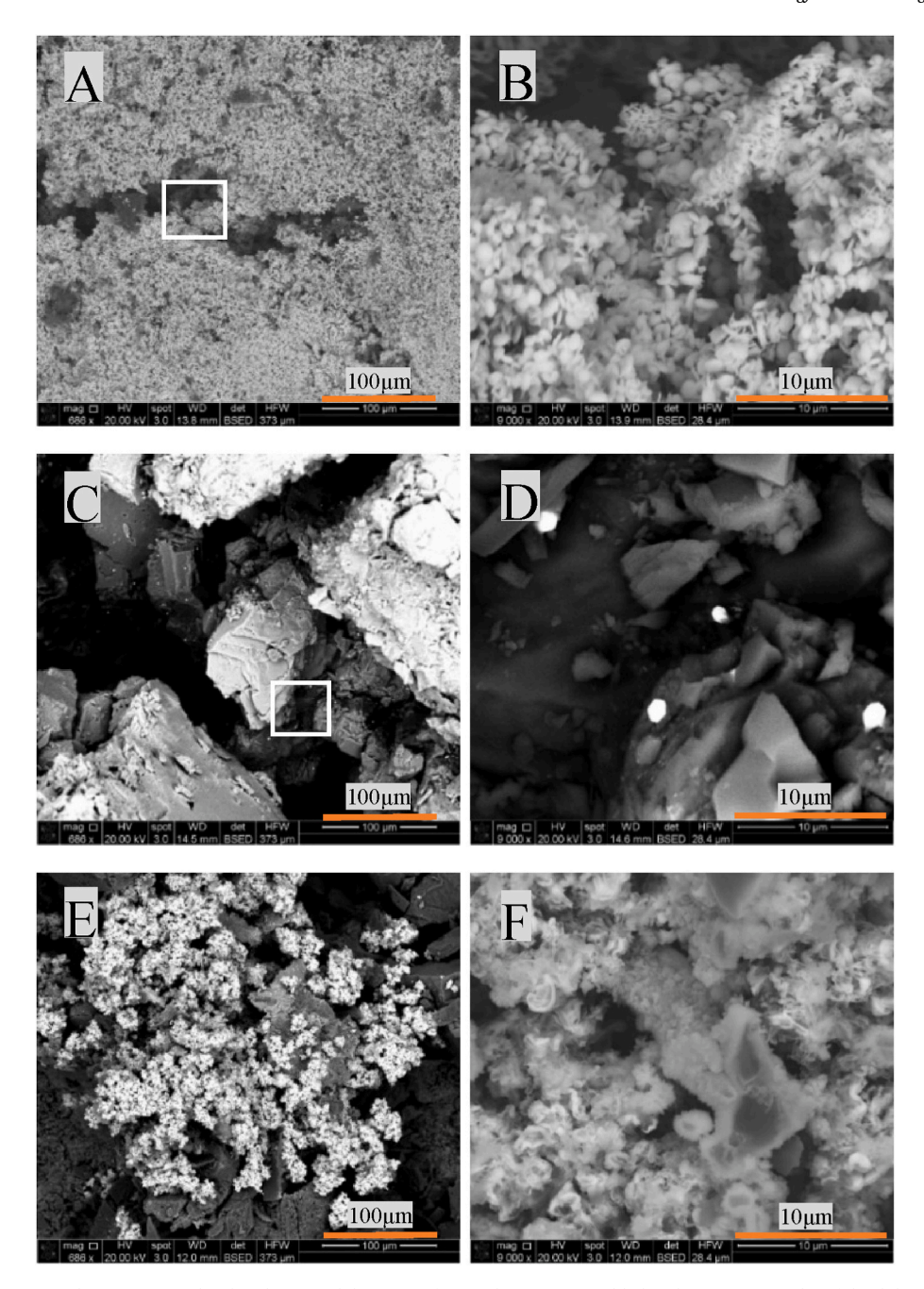


Fig. 8. SEM images of toxic metals precipitates (bright white) on dolomite surface with FW type I (added with CaCO<sub>3</sub>): A) Inlet of the dolomite core, B) Zoom-in of A showing precipitates of different shapes and sizes, C) Center of the dolomite core showing hexagonal-shaped precipitates, D) zoom-in of C, E) Outlet of the dolomite core showing huge bright patches of precipitates, and F) zoom-in of E showing precipitates with irregular shapes.

where Me is Ca and Mg, Ms is Ca, Mg, Ba, Sr, Cd, and Pb, and >MeOH $^{\rm O}$  and >CO $_3$ H $^{\rm O}$  are the hydration sites of dolomite. The dissolution of dolomite in the conducted experiments is reflected by an increase in the concentration of Ca and Mg. The increase is larger with PW that was not supplied with CaCO $_3$  to increase alkalinity and acidic pH (Tables S3, S4, S5, and S6).

Representative precipitation reaction:

$$Ms^{2+} + CO_3^{2-} \leftrightarrow MsCO_3$$
 (5)

According to this reaction mechanism, during the initial stages  $(0-125\,\text{mL})$ , the initial alkalinity and pH of PW controlled the removal of toxic metals by sorption and precipitation reactions (Eq. (3) – (5)). This is reflected by a fast increase of all toxic metal removal. Dolomite

dissolution which takes place concomitantly with sorption and precipitation reactions (Eq. (1)) resulted in an increase of pH from 6.9 to  $\sim\!7.6$  and alkalinity from 102 to 114 mg/L (Eq. (3)). An increase of alkalinity promoted the continuous removal of some toxic metals such as Pb (Eq. (5)) whose removal is mostly due to precipitation reactions, but attenuated the removal of some toxic metals such as Ba and Sr whose removal is mostly by sorption reactions (Omar and Vilcáez, 2023). Precipitation of toxic metals is reflected by a drop of alkalinity from 114 to 85 mg/L, and the attenuation of sorption reactions are reflected by a decrease of Ba, Sr, Cd, and As removal (125–250 mL). Eventually, during the later stages (>250 mL) of the flooding process, pH and alkalinity reach a steady condition controlled by the dissolution of dolomite. This is reflected by practically a constant rate of toxic metals removal by sorption and precipitation reactions. Apparently, dolomite dissolution favors

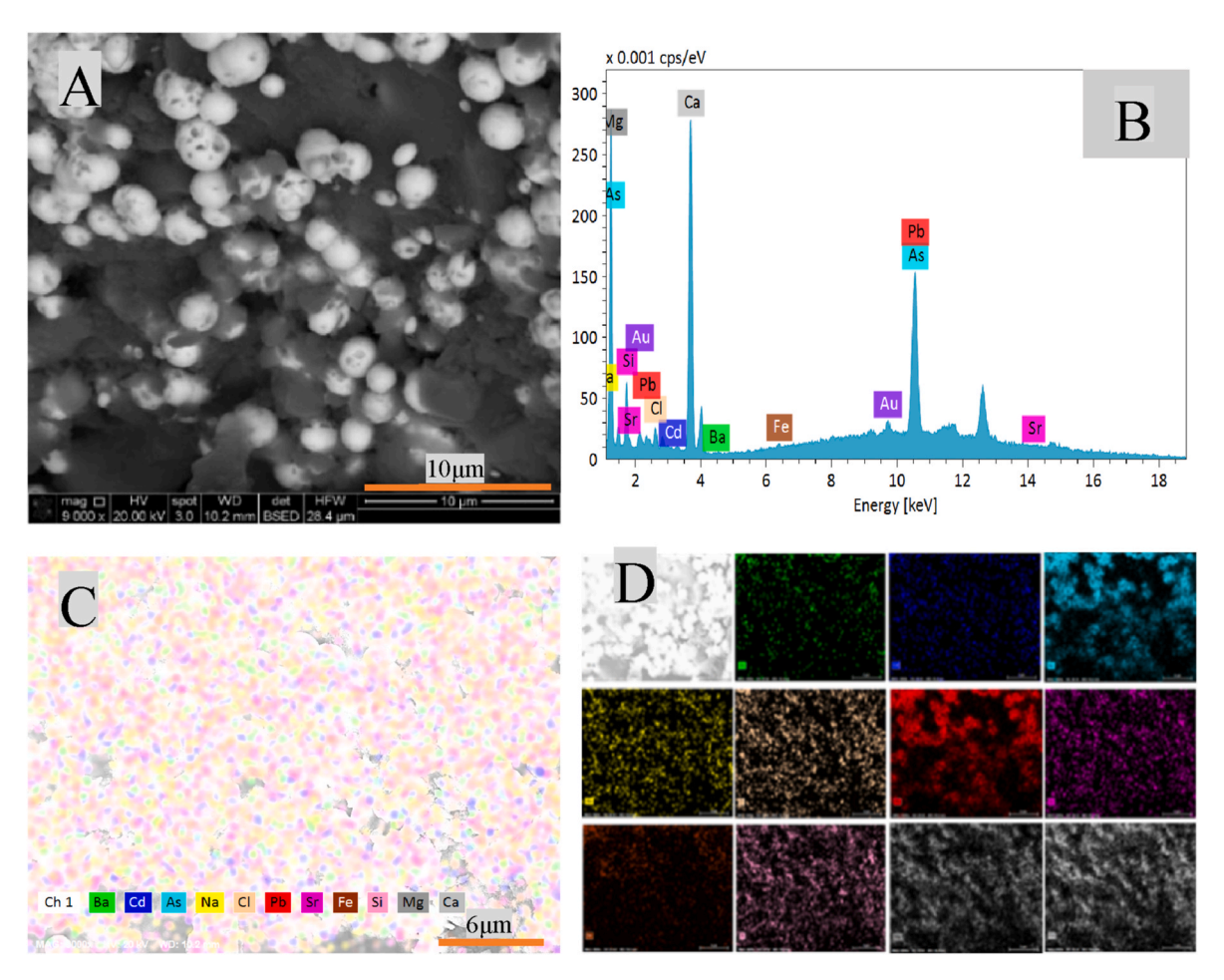


Fig. 9. SEM-EDS mapping of toxic metals on dolomite surface with PW type II (added with CaCO<sub>3</sub> to increase alkalinity) at the inlet of the dolomite core: A) SEM micrograph showing carbonate precipitates with rounded to oval shapes in the cavities of the dolomite surface, B) EDS spectrum showing the elemental composition of the bulk sample, C) EDS mapping of metals, and D) EDS mapping layers of individual elements.

precipitation reactions by increasing alkalinity (and thus pH), but it opposes sorption reactions by increasing the concentration of cations (Ca and Mg) that compete for the hydration sites of dolomite.

To verify the effect of dolomite dissolution on the removal of toxic metals under flow conditions, we repeated the experiments using a shorter synthetic dolomite core (8.2 cm length). Fig. 3 shows Ba, Sr, Cd, Pb, and As removal profiles, as well as total alkalinity concentration and pH profiles at the outlet of a dolomite core (8.2 cm length) injected with PW type II of 79.6 mg/L total alkalinity (Table 1). During the initial stages (0-125 mL), removal levels of toxic metals obtained with a dolomite core of 8.2 cm length (Fig. 3) were practically the same removal levels obtained with a dolomite core of 16.9 cm (Fig. 2), confirming that initially the removal of toxic metals by dolomite is controlled by the initial alkalinity and pH of PW. However, the removal levels decreased during the later stages (>125 mL) where dolomite dissolution controlled the removal of toxic metals. The decrease is larger with shorter dolomite core (8 cm length) than with a larger dolomite core (16.9 cm length), confirming that the amount of alkalinity generated from the dissolution of dolomite plays an important role in the removal of toxic metals by dolomite. Dolomite dissolution ends up controlling both sorption and precipitation reactions according to the described reaction mechanism (Eqs. (1)–(5)). Consequently, the larger the size of the dolomite core, the larger the removal levels of toxic metals that can be achieved. This finding has practical implications to predict the transport toxic metals in PW disposed in deep saline aquifers as well as to design dolomite filters to remove toxic metals from PW on the surface.

Given the fact that alkalinity in PW is variable and that some PW have close to zero alkalinity, we conducted experiments using PW type III that was not added with CaCO<sub>3</sub> to increase alkalinity. Fig. 4 shows Ba, Sr, Cd, Pb, and As removal profiles, as well as total alkalinity concentration and pH profiles at the outlet of the dolomite core (15.8 cm length) injected with PW type III of total alkalinity below detection limits (Table 1). The initial pH of PW type III was acidic due to the formation of hydrochloric acid according to the following reaction:  $AsCl_3 + 3H_2O = As(OH)_3 + 3HCl$ . The formed acid resulted in a pH of  $\sim$ 2.4. The fast dissolution of dolomite under acidic conditions (Eq. (1)), resulted in a fast increase of pH to ~7.5 and remained practically constant throughout the remainder of the experiment. Like the removal profiles obtained with PW type I whose initial alkalinity was increased by adding CaCO<sub>3</sub>, removal levels of toxic metals with PW type III (Fig. 4) reached highest levels during the initial stages of the flooding process (0-125 mL) where alkalinity generated from the dissolution of dolomite controlled the removal of Ba, Sr, Cd, As, and Pb. Apparently, the acidic pH of PW type III, resulted in a fast dissolution rate of dolomite which provides alkalinity for the precipitation of metals (Eq. (5)). However, given the high concentration of protons (H<sup>+</sup>) which also compete for hydration sites of dolomite (Eqs. (3) and (4)), attained removal levels of Ba, Sr, and Cd whose removal is mostly due to sorption reactions, reached lower levels with PW type III than with PW type I. Fluctuations in the removal of toxic metals following the initial stages (>125 mL) might be due to fluctuations between the stages controlled by sorption/ precipitation reactions and dolomite dissolution reactions.

To further investigate the role of dolomite dissolution and alkalinity

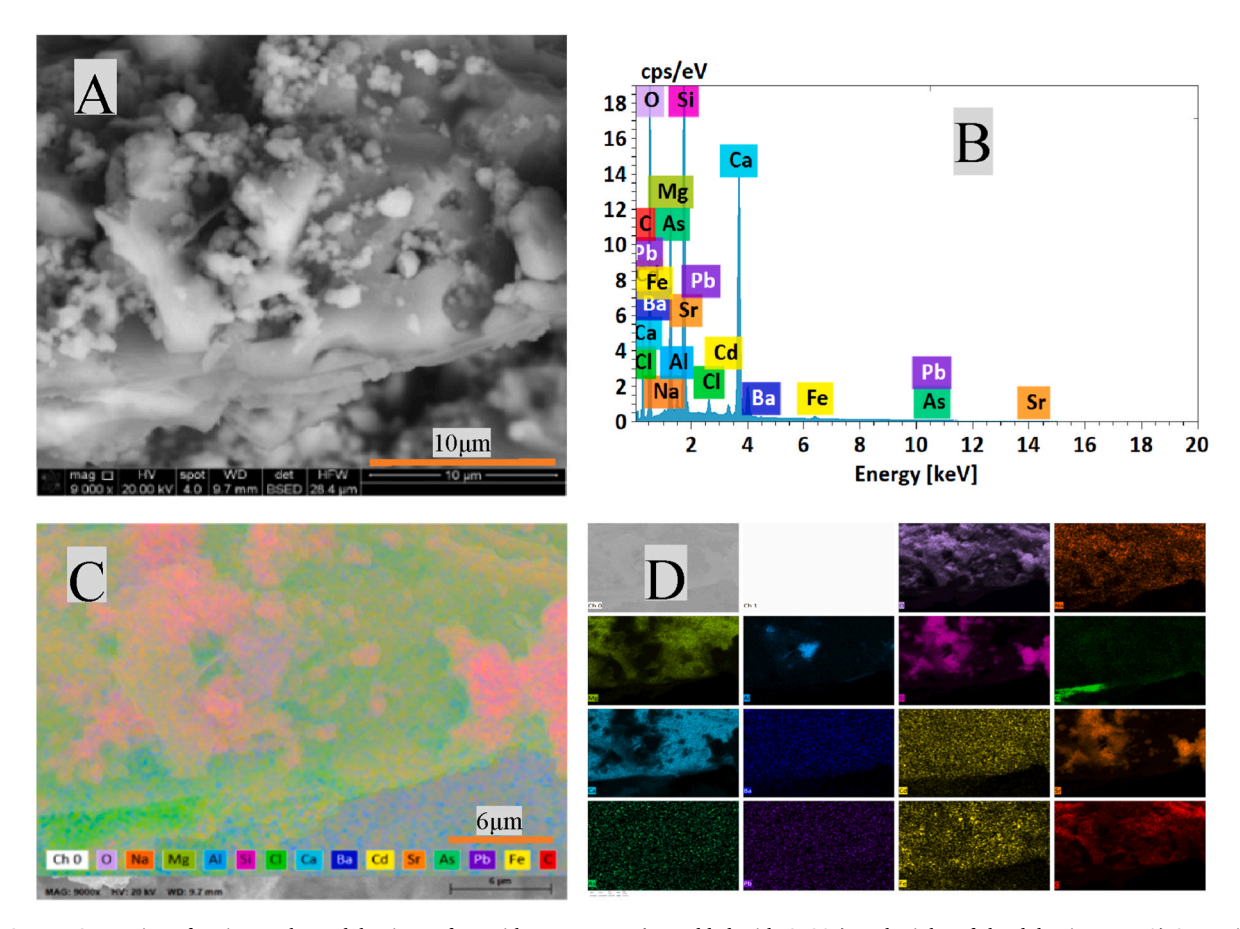


Fig. 10. SEM-EDS mapping of toxic metals on dolomite surface with PW type IV (not added with CaCO<sub>3</sub>) at the inlet of the dolomite core: A) SEM micrograph showing carbonate precipitates, B) EDS spectrum showing the elemental composition of the bulk sample, C) EDS mapping of metals, and D) EDS mapping layers of individual elements.

on the removal of toxic metals, we repeated the previous experiment using PW type IV which was not supplied with CaCO<sub>3</sub> using a shorter dolomite core (8.1 cm length). Fig. S2 shows Ba, Sr, Cd, Pb, and As removal profiles, as well as total alkalinity concentration, and pH profiles at the outlet of the dolomite core injected with PW type IV of total alkalinity below detection limits (Table 1). The profiles are like those obtained using a shorter dolomite core, and as expected, lower removal levels were attained for Ba, Sr, Cd, and As using a 8.1 cm length than a 16.2 cm length dolomite core, confirming that dolomite dissolution favors toxic metals removal by increasing alkalinity and pH of PW.

Another important goal of this study was to identify differences between the removal of toxic metals by dolomite from PW and FW. To this aim, we conducted core-flooding experiments using FW (Table 2) instead of PW (Table 1). Fig. 5 shows Ba, Sr, Cd, Pb, and As removal profiles, as well as total alkalinity concentration and pH profiles at the outlet of the dolomite core injected with FW type I of 2.8 mg/L total alkalinity (see Table 4).

In accordance with previous studies showing the inhibitory effect of chloro complexation reactions on the sorption of metals in dolomite (Omar and Vilcáez, 2022) according to:  $Ms^{2+} + 2Cl^- \leftrightarrow (MsCl_2)^+$ , which reduces the concentration of free dissolved cations in solution that can form surface complexes with dolomite (Eqs. (3) and (4)), higher removal levels of toxic metals were obtained with FW than with PW. However, considering the higher amounts of alkalinity generated from the dissolution of dolomite observed with FW type I (210 mg/L) than with PW type I (115 mg/L) during the initial stages of the flooding process, higher removal levels of toxic metals during the initial stages from FW than from PW are attributed to the precipitation reactions driven by the dissolution of dolomite. Apparently, dolomite dissolution is faster with FW than with PW and the competition of Na for hydration sites might

have played a role.

The larger drop of Ba, Sr, and Cd removal with FW than with PW in the later stages of the flooding process (>250 mL) where alkalinity concentration decreases, can also be attributed to the competition of cations for hydration sites. In addition to alkalinity, dolomite dissolution (Eq. (1)), increases the concentration of Ca and Mg in the aqueous phase. With low chloride and alkalinity concentrations in the aqueous phase, the high concentrations of free Ca and Mg ions outcompetes Ba, Sr, and Cd for hydration sites. This behavior was particularly relevant for Cd. A decrease in alkalinity during the latest stage due to precipitation reactions was accompanied by a decrease in the removal levels of Cd. Similar behavior and toxic metals removal was observed using FW type II (Fig. S3) that was not added with CaCO3 to increase the initial alkalinity.

#### 4.2. SEM analysis of dolomite surface

Fig. 6 shows representative BSEs-SEM images comparing the surface morphology of dolomite grains collected from the inlet of dolomite cores injected with PW type II (without added CaCO<sub>3</sub>) and FW II (without added CaCO<sub>3</sub>). The surface morphology of dolomite changed after the core-flooding experiment owing to the dissolution of dolomite and carbonate minerals precipitation. The dissolution of dolomite resulted in rough surface morphology and porosity development. Precipitates had different shapes, roundness, and size. The shapes of precipitates ranged from circular, oval, and polygonal to irregular forms with smooth perfect to etched angular roundness. The size of precipitates ranged from several nanometers to several micrometers. The largest size precipitates were observed at the inlet of the dolomite core. Precipitates were commonly seen with cavities or as partially eroded particles, especially

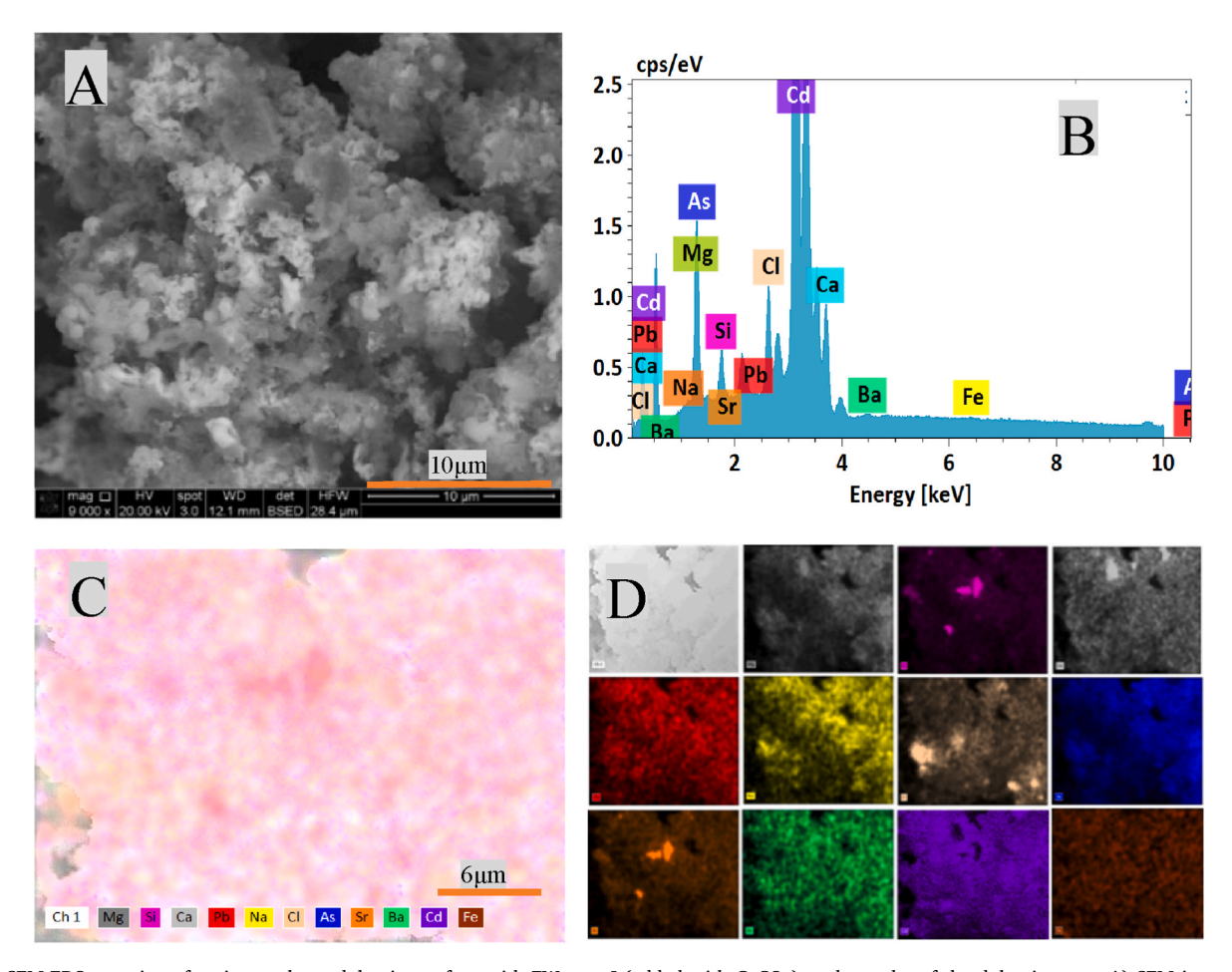


Fig. 11. SEM-EDS mapping of toxic metals on dolomite surface with FW type I (added with CaCO<sub>3</sub>) at the outlet of the dolomite core: A) SEM image showing carbonate precipitates on the dolomite surface, B) EDS spectrum showing the elemental composition of the bulk dolomite sample, C) EDS mapping of metals, and D) EDS mapping layers of individual elements.

with PW. The deposition and arrangement of precipitates were different from place to place within the same dolomite core. Precipitates were found as single particles mainly at the center of the dolomite core whereas precipitates at the inlet and outlet of the dolomite core were mainly clustered to clumped precipitates. The number of precipitates was significantly larger in locations surrounding the pore troughs on edges and cavities, and on grain surfaces facing the fluid flow direction. The nature and composition of these precipitates are discussed in the following sections.

Figs. 7 and 8 show metal precipitates at the inlet, center, and outlet of dolomite cores ( $\sim$ 8 cm length) with PW type I and FW type I which were added with CaCO3 to increase alkalinity. The much larger amounts of precipitates at the three points with FW type I than with PW type I, confirms the different solubility of metals at low and high salinity (ionic strength) conditions. This is particularly evident at the inlet of the dolomite core injected with FW type I where dolomite surface was practically completely covered precipitates. A similar behavior was observed with PW and FW that were not added with CaCO3 to increase alkalinity (Figs. S4 and S5) and the amounts of precipitates decreased with decreasing alkalinity. Confirming that besides salinity, alkalinity plays a role in the removal of toxic metals by dolomite.

## 4.3. SEM-EDS analysis of dolomite surface

To identify the elemental composition of the precipitated and sorbed phases in the dolomite cores flooded with PW and FW, we mapped the elemental composition of dolomite grain surfaces by SEM-EDS analysis. Figs. 9–11 show SEM-EDS images of dolomite grains after the dolomite

cores were flooded with 1 L of PW type II (added with CaCO<sub>3</sub>), PW type IV (not added with CaCO<sub>3</sub>), and FW type I (added with CaCO<sub>3</sub>), respectively. The presence of Ba, Sr, Cd, Pb, and As in the spectra confirms their removal from PW and FW. A cross-matching between the map of each element and the SEM images of precipitates reveals that precipitates of heavy metals (Pb) and metalloids (As) are more abundant than precipitates of alkaline earth metals (Ba and Sr). This agrees with the removal levels of Sr and Ba which were relativity smaller than the removal levels of Cd, Pb, and As. A comparison between the SEM-EDS images and spectrum for PW types II and IV confirms that the amount of precipitates increases with increasing alkalinity, and that the shapes of precipitates can be different depending on the available alkalinity. Whereas a comparison between the SEM-EDS images and spectrum of PW type II and FW type I confirms the highest removal of Cd from FW than from PW is due to precipitation and coprecipitation reactions. Similar conclusions can be drawn by comparing the SEM-EDS images and spectrum of PW type I and FW type II (Figs. S6 and S7). Sr was found in sorbed and coprecipitated phases, and it was predominantly associated with other metals in the precipitates. In accordance with the relatively low levels of Sr removal observed in the experiments, Sr precipitates were less frequently found than other toxic metal precipitates. Ba was found as sorbed and coprecipitated phases. Ba precipitates showed polygonal to irregular shapes of 2-4 µm size that precipitated in the cavities of dolomite surface or between dolomite crystals (Fig. S7). Pb precipitates were commonly found inside dints or at edges of dolomite grains/crystals (Fig. S5). Pb precipitates occurred as cluster and clumped oval shape precipitates of nano to micro scale size. Moreover, Pb and As were commonly found in precipitates close to the

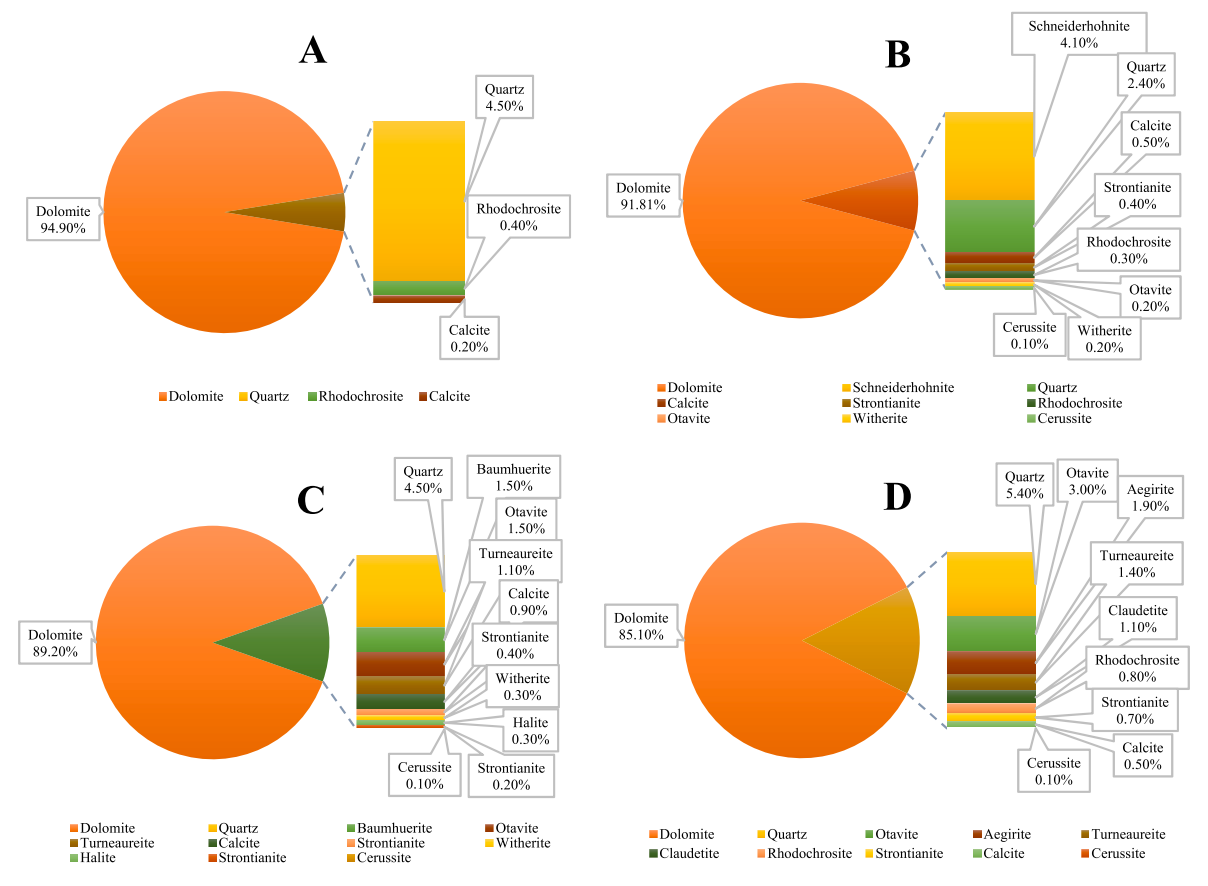


Fig. 12. Semiquantitative analyses from high-resolution XRD (Fig. S8) conducted on the powdered dolomite samples collected from dolomite core flooded with PW type I: A) Control sample, B) Inlet, C) Center, and D) Outlet.

inlet of the dolomite core. This behavior suggests that the precipitation rates of Pb and As are faster than the precipitation rates of Ba, Sr, and Cd that precipitates away from the inlet point. Overall, SEM-EDS analysis confirms that the removal of Ba and Sr from PW is controlled by sorption reactions with minor precipitation/coprecipitation reactions. However, the removal of Pb and As, and thus their transport by PW in dolomite, is mainly controlled by precipitation/coprecipitation reactions.

#### 4.4. XRD analysis of precipitates

To elucidate whether the observed precipitates were crystalized carbonates and to determine their distribution through the dolomite core, we conducted high-resolution XRD analyses. Figs. 12 and 13 show all the minerals detected through semiquantitative analysis of highresolution XRD data. Analysis was done on samples collected from the inlet, center, and outlet of the dolomite core after being flooded with 1 L of PW or FW, as well as on a control dolomite sample collected before preparing the dolomite cores. The major minerals in the control dolomite sample were dolomite and quartz. However, XRD spectra showed minor content of silica (quartz) and ankerite, as well as traces of other carbonate minerals (calcite and rhodochrosite) in some control samples. Various carbonate minerals and oxide phases were detected in the collected dolomite grains, confirming that these minerals precipitated during the core-flooding experiments. The type and amount of minerals detected by XRD analysis are considerably distinct from sample to sample.

The composition of the precipitated minerals corresponds to the chemical composition of the employed types of PW and FW. For example, carbonate minerals phases detected in dolomite cores flooded with PW type I-IV are witherite (BaCO $_3$ ), strontianite (SrCO $_3$ ), otavite (CdCO $_3$ ), cerussite (PbCO $_3$ ), and arsenic phases (e.g., As $_2$ O $_3$ )

(Figs. S8–S10), which are known to be more thermodynamically stable at standard conditions (Antao et al., 2009). In addition to these minerals, calcite, vaterite, and specific polymetallic oxides were also detected but aragonite was never detected. Detected oxide phases were largely arsenate minerals and coprecipitated arsenate phases such as schneiderhohnite (As<sub>5</sub>Fe<sub>4</sub>O<sub>13</sub>) and lead arsenate (PbAs<sub>2</sub>O<sub>4</sub>). As oxides were detected in samples collected from experiments using both synthetic PW and FW. As is known to form oxide phases in aqueous environments (Neuberger and Helz, 2005) and to coprecipitate with carbonate minerals during their transformation from hydrated (e.g., monohydrocalciteto) to anhydrous (e.g., calcite and aragonite) carbonate phases in saline water (Fukushi et al., 2011).

The amount of Pb and As carbonate/oxide phases were generally high at the inlet of the core and decreased at the center and outlet of the dolomite core. Conversely, the amounts of Ba and Sr carbonate minerals were low at the inlet of the core and increased at the center and outlet of the dolomite core. On the other hand, the amount of Cd carbonate minerals was low or absent at the inlet and gradually increased at the center, reaching a maximum at the outlet of the dolomite core. Sorption/precipitation of Pb and As occurred preferentially closer to the inlet while sorption/precipitation of Ba, Sr, and Cd occurred preferentially away from the inlet of the dolomite core. This is attributed to their different chemical equilibrium and reaction kinetics.

#### 5. Conclusions

The obtained results suggest the following mobility of the tested toxic metals in dolomite: Sr>Ba>Cd>As>Pb. Based on the obtained results from SEM, SEM-EDS, and XRD analyses, all tested toxic metals undergo precipitation and sorption reactions. However, the removal by dolomite and thus the transport of Ba and Sr in dolomite is mainly

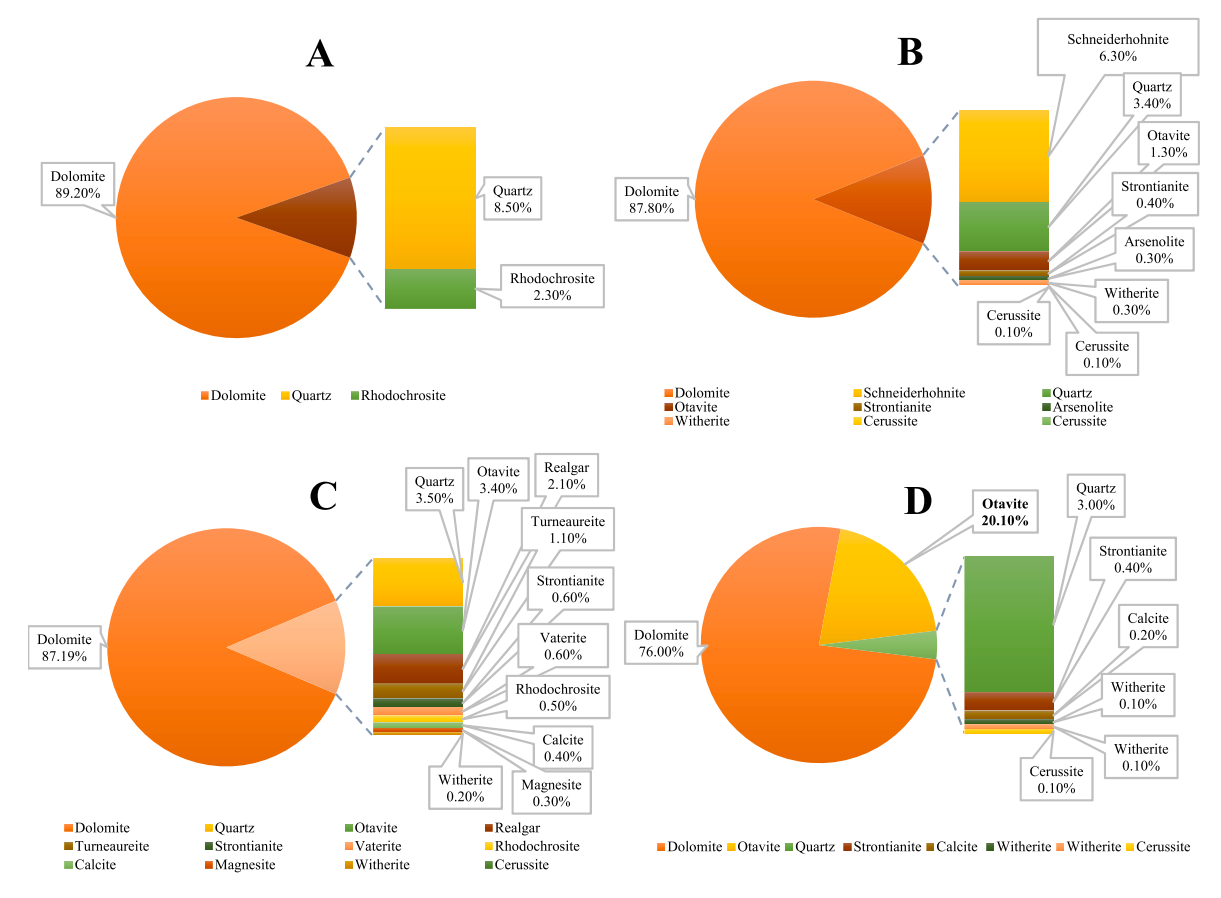


Fig. 13. Semiquantitative analyses from high-resolution XRD (Fig. S9) conducted on the powdered dolomite samples collected from dolomite core injected with FW type II: A) Control sample, B) Inlet sample, C) Center sample, and D) Outlet sample.

controlled by nonequilibrium sorption reactions while the transport of Pb and As is predominantly controlled by precipitation and/or coprecipitation reactions of carbonate minerals. Cd removal is controlled by sorption and/or precipitation reactions depending on the alkalinity and pH of PW. Toxic metals (Ba, Sr, Cd, As, and Pb) precipitate as carbonate minerals such as witherite (BaCO<sub>3</sub>), strontianite (SrCO<sub>3</sub>), otavite (CdCO<sub>3</sub>), cerussite (PbCO<sub>3</sub>), and arsenic phases (e.g., As<sub>2</sub>O<sub>3</sub>) that are associated with calcite, vaterite, and polymetallic oxides. They precipitate preferentially in locations surrounding the pore throats, on grain edges and cavities, and on grain surfaces that are facing the fluid flow direction. Sorption and precipitation of Pb and As occurs preferentially at the injection point of PW into dolomite while precipitation and sorption reactions of Ba, Sr, and Cd takes place preferentially in locations away from the inlet point, indicating that Pb and As undergo faster removal rates than Ba, Sr, and Cd in dolomite. Overall, these new results reveal a key role of alkalinity of PW and dolomite dissolution in promoting the removal of toxic metals from PW via precipitation/coprecipitation and/or sorption reactions, which in turn retards their transport in dolomite.

#### **Funding**

This work was supported by the National Science Foundation under Grant CBET-220036.

#### **Declaration of interests**

The authors declare that they have no known competing financial interests or personal relationships that could have appeared to influence the work reported in this paper.

#### CRediT authorship contribution statement

**Khalid Omar:** Investigation, Methodology, Writing – original draft. **Javier Vilcáez:** Conceptualization, Supervision, Funding acquisition, Writing – review & editing.

#### Data availability

No data was used for the research described in the article.

#### Acknowledgments

This is Oklahoma State University Boone Pickens School of Geology contribution number 2023-138.

# Appendix B. Supplementary data

Supplementary data to this article can be found online at https://doi.org/10.1016/j.geoen.2023.212342.

#### References

Alomar, T.S., Hameed, B.H., Usman, M., Almomani, F.A., Ba-Abbad, M.M., 2022. Recent advances on the treatment of oil fields produced water by adsorption and advanced oxidation processes. Journal of Water Process Enginneering 49, 103034.

Antao, M., Sytle, Hassan, I., 2009. The orthorhombic structure of CaCO3, SrCO3, PbCO3 and BaCO3: linear structural trends. Can. Mineral. 47, 1245–1255.

Ballinger, D.G., 1979. Methods for chemical analysis of water and wastes. In: United States Environmental Protection Agency. Environmental Monitoring and Support Labotatory Cincinnati, Ohio, 1979.

Dixit, S., Hering, J.G., 2003. Comparison of arsenic (V) and arsenic (III) sorption onto iron oxide minerals: implications for arsenic mobility. Environ. Sci. Technol. 37 (18), 4182–4189.

- Drever, J.I., 1997. The geochemistry of natural waters: surface and groundwater environments 436, p87–p105.
- Ebrahimi, P., Vilcáez, J., 2018a. Effect of brine salinity and guar gum on the transport of barium through dolomite rocks: implications for unconventional oil and gas wastewater disposal. J. Environ. Manag. 214, 370–378.
- Ebrahimi, P., Vilcáez, J., 2018b. Petroleum produced water disposal: mobility and transport of barium in sandstone and dolomite rocks. Sci. Total Environ. 634, 1054–1063.
- Ebrahimi, P., Vilcáez, J., 2019. Transport of barium in fractured dolomite and sandstone saline aquifers. Sci. Total Environ. 647, 323–333.
- Federation, W.E., Aph Association, 2005. Standard Methods for the Examination of Water and Wastewater. American Public Health Association (APHA), Washington, DC, USA, 4-75 to 4-76 (chloride method 4500-Cl G) and 4-127 to 4-129 (nitrate method 4500-NO3 I).
- Fukushi, K., Munemoto, T., Sakai, M., Yagi, S., 2011. Monohydrocalcite: a promising remediation material for hazardous anions. Sci. Technol. Adv. Mater. 12 (6), 064702
- Guerra, K., Dahm, K., Dundorf, S., 2011. Oil and Gas Produced Water Management and Beneficial Use in the Western United States. US Department of the Interior, p. 157.
- Jensen, J., 2020. The Role of Carbonate Minerals in Arsenic Mobility in a Shallow Aquifer Influenced by a Seasonally Fluctuating Groundwater Table. Masters thesis, Utah State University.
- Jiménez, S., Micó, M.M., Arnaldos, M., Medina, F., Contreras, S., 2018. State of the art of produced water treatment. Chemosphere 192, 186–208.
- Kharaka, Y.K., Kakouros, E., Thordsen, J.J., Ambats, G., Abbott, M.M., 2007. Fate and groundwater impacts of produced water releases at OSPER "B" site, Osage County, Oklahoma. Appl. Geochem. 22 (10), 2164–2176.
- Neuberger, C.S., Helz, G.R., 2005. Arsenic (III) carbonate complexing. Appl. Geochem. 20 (6), 1218–1225.

- Omar, K., Vilcáez, J., 2022. Removal of toxic metals from petroleum produced water by dolomite filtration. J. Water Proc. Eng. 47, 102682.
- Omar, K., Vilcáez, J., 2023. The Role of Alkalinity on Toxic Metals Removal from Petroleum Produced Water by Dolomite. Applied Geochemsitry.
- Pokrovsky, O.S., Schott, J., Thomas, F., 1999. Processes at the magnesium-bearing carbonates/solution interface. I. a surface speciation model for magnesite. Geochem. Cosmochim. Acta 63 (6), 863–880.
- Ribeiro, L.P.S., Puchala, R., Lalman, D.L., Goetsch, A.L., 2021. Composition of various sources of water in Oklahoma available for consumption by ruminant livestock. Applied Animal Science 37 (5), 595–601.
- Saha, S., et al., 2020. Microbial symbiosis: a network towards biomethanation. Trends Microbiol. 28 (12), 968–984.
- Tabatabaeefar, A., Yuan, Q., Salehpour, A., Rajabi-Hamane, M., 2020. Batch adsorption of lead (II) from aqueous solution onto novel polyoxyethylene sorbitan monooleate/ ethyl cellulose microfiber adsorbent: kinetic, isotherm and thermodynamic studies. Separ. Sci. Technol. 55 (6), 1051–1061.
- Temple, B.J., Bailey, P.A., Gregg, J.M., 2020. Carbonate Diagenesis of the Arbuckle Group North Central Oklahoma to Southeastern Missouri, pp. 10–30.
- Vilcáez, J., 2020. Reactive transport modeling of produced water disposal into dolomite saline aquifers: controls of barium transport. J. Contam. Hydrol. 233, 103600.
- Walsh 3rd, F.R., Zoback, M.D., 2015. Oklahoma's recent earthquakes and saltwater disposal. Jun 18 Sci. Adv. 1 (5), e1500195, 10.1126/sciadv.1500195. PMID: 26601200; PMCID.
- Wei, H., Shen, Q., Zhao, Y., Wang, D.J., Xu, D.F., 2003. Influence of polyvinylpyrrolidone on the precipitation of calcium carbonate and on the transformation of vaterite to calcite. J. Cryst. Growth 250 (3–4), 516–524.
- Yin, X., et al., 2019. Co-transport of graphene oxide and heavy metal ions in surfacemodified porous media. Chemosphere 218, 1–13.